Airflow velocity effects on air bearing with grooved disk surface in near-field optical disk drives

H. C. Wang and T. S. Liu

Citation: Physics of Fluids (1994-present) **18**, 057103 (2006); doi: 10.1063/1.2194072
View online: http://dx.doi.org/10.1063/1.2194072
View Table of Contents: http://scitation.aip.org/content/aip/journal/pof2/18/5?ver=pdfcov
Published by the AIP Publishing

Articles you may be interested in

Direct near-field optical investigation of phase-change medium in blue-ray recordable and erasable disk
Appl. Phys. Lett. **95**, 103105 (2009); 10.1063/1.3222901

Super-resolution near-field optical disk with an additional localized surface plasmon coupling layer
J. Appl. Phys. **91**, 10209 (2002); 10.1063/1.1476068

1.5-Mbit/s direct readout of line-and-space patterns using a scanning near-field optical microscopy probe slider with air-bearing control
Appl. Phys. Lett. **76**, 804 (2000); 10.1063/1.125590

Transmitted signal detection of optical disks with a superresolution near-field structure
Appl. Phys. Lett. **75**, 151 (1999); 10.1063/1.124302

Near-field optical recording on the cyanine dye layer of a commercial compact disk-recordable
J. Vac. Sci. Technol. A **15**, 1442 (1997); 10.1116/1.580558

This article is copyrighted as indicated in the article. Reuse of AIP content is subject to the terms at: http://scitation.aip.org/termsconditions. Downloaded to IP: 140.113.38.11 On: Thu, 01 May 2014 02:01:24

Airflow velocity effects on air bearing with grooved disk surface in near-field optical disk drives

H. C. Wang and T. S. Liu
Department of Mechanical Engineering, National Chiao Tung University, Hsinchu 30010, Taiwan, Republic of China

(Received 19 October 2005; accepted 10 March 2006; published online 5 May 2006)

By means of an air bearing, the pickup head slider of a near-field optical disk drive flies above data tracks on a rotating disk surface to achieve a stable flying height. The influence of airflow velocities of the air bearing on lift force deserves investigation, as the airflow velocity varies during track seeking or disk speed variation. In this study, a direct simulation Monte Carlo method is used to investigate three-dimensional nanoscale gas film lubrication at the air bearing between a slider and a rotating disk. This study aims to investigate air bearing behavior at different airflow velocities. Computational results show that faster flow generates larger pressure and lift force. Lower flying height reduces force variation caused by different velocities. This study also proposes a method for maintaining the flying height within the near-field range. © *2006 American Institute of Physics*. [DOI: 10.1063/1.2194072]

I. INTRODUCTION

To increase data storage density and capacity for multimedia and information technology, near-field optical disk drives represent one of promising devices.[1,2] For the sake of near-field optics, an optical pickup head slider has to fly above the disk surface at a distance smaller than the mean free path of molecules in the air, i.e., 65 nm at standard atmospheric pressure (STP).

The disk surface under rotation gives rise to airflow, which creates air pressure and provides lift force at the head/disk interface. Traditionally, macroscopic hydrodynamic equations, e.g., Reynolds equations and Navier-Stokes equations are used to deal with the macroscopic flow behavior. In gas film lubrication problems under submicron or less clearance conditions, flow in the gas films cannot be dealt with as continuum flows because the molecular mean free path is not negligible compared to the clearances. Accordingly, they must be treated as rarefied gas flows based on kinetic theory.[3] One of the most important parameters in the kinetic theory is Knudsen numbers, which are defined as the ratio of the molecular mean free path to the characteristic length. Burgdorfer[4] introduces the concept of the kinetic theory to the field of gas film lubrication and uses a slip flow velocity boundary condition.

A statistics-based method, the direct simulation Monte Carlo (DSMC) method presented by Bird[5] in the early 1970s, can predict the airflow behavior. The DSMC method is capable of dealing with air bearing problems when the slider and disk quasicontact or contact. Alexander *et al.*[6] validated DSMC by comparing with Reynolds equation results in rarefied gas. Huang and Bogy[7,8] proved that the DSMC method and the modified Reynolds equations yield similar results in the range of Knudsen number up to 6 for minimum spacing of 10 nm. Their simulation results were compared with a slip correction for Reynolds equation, based on the Boltzmann equation. The modified Reynolds equation was introduced by Fukui and Kaneko[9] where the Poiseuille flow rate was calculated on the basis of a linearized Bhatnagar-Gross-Krook model[10] of the Boltzmann equation. Slider posture effects on the air bearing in hard disk drives were examined by Liu and Ng.[11] For near-field optical disk drives, Wang *et al.*[12] investigated effects of disk surface grooves and compared with results without grooves, according to which the presence of the groove reduces the pressure at the head/disk interface.

A pickup head slider undergoes two motions when flying above a disk. One is track following, in which the slider flies above the disk at the same radial position to read continuous data. The other is track-seeking motion, which occurs in searching data on the disk. To facilitate data reading/writing, stable lift force during track seeking is desired, as lift force variation degrades stability. This study investigates the air bearing for a slider flying above the near-field optical disk at different speeds. The DSMC method is used to develop the air bearing model for pressure distributions in head/disk interface at the same position of different disk speeds or at different positions of the same disk speed. This study also concerns the lift force change percentage when airflow velocity changes or slider flying height changes. The pressure change percentage can represent stability in track seeking and track following.

II. DSMC METHOD

The air bearing force and flying height analysis are crucial for air bearing design. In this study, the flying pickup head slider flies within the range of the mean free path of air molecules λ ($\lambda=65$ nm at STP for air). Unfortunately, continuum assumption begins to break down when the molecular mean free path λ becomes comparable to flow characteristic length L. The ratio of these two quantities is known as the Knudsen number ($\mathrm{Kn}=\lambda/L$) and is usually used to indicate the degree of rarefaction. Based on the Knudsen number, flows are divided into four categories:[1,3] $\mathrm{Kn}<0.01$ (con-

 © 2006 American Institute of Physics

This article is copyrighted as indicated in the article. Reuse of AIP content is subject to the terms at: http://scitation.aip.org/termsconditions. Downloaded to IP: 140.113.38.11 On: Thu, 01 May 2014 02:01:24

tinuum), $0.01<\mathrm{Kn}<0.1$ (slip flow), $0.1<\mathrm{Kn}<3$ (transitional flow), and $\mathrm{Kn}>3$ (free molecular flow). Kn values in this study range from 1.625 to 3.25, corresponding to flying heights from 40 to 20 nm. Hence, the flow in this study belongs to the transitional flow and free molecular flow. This study uses the DSMC method to deal with those rarefied gas problems.

The basic idea of DSMC is to calculate airflows by using the physical foundation rather than mathematical foundation. The assumptions of molecular chaos and dilute air are required in both the Boltzmann formulation and the DSMC method. Molecules move in the simulated physical domain so that the physical time is a parameter in simulation and all flows are computed as unsteady flows. An important feature of DSMC is that the molecular motion and the intermolecular collisions are uncoupled over time intervals that are much smaller than the mean collision time. Both the collision between molecules and the interaction between molecules and solid boundaries are computed on a probabilistic basis. Unlike molecular dynamics methods, the DSMC method provides probability and average physical quantities instead of predicting the instantaneous state of each air molecular particle. In practice, the number of simulated molecules is extremely small compared with the number of real molecules.

Air molecule inflow and outflow in a simulation region are hard to predict. In order to perform simulation with inflow/outflow pressure boundaries, a general procedure for these conditions by using the concept of particle flux conservation has been developed.[5] Applying particle flux conservation is the basic idea to update the inflow and outflow velocities. At each pressure boundary, the mass flow rate conserves automatically and simulated boundary pressures coincide with the imposed values by assuming thermal equilibrium.

The molecule position in the simulation region is assumed of Maxwellian distribution,[5] which is written as a function of molecular thermal velocity v; i.e.,

$$f(v)=\left(\frac{\beta}{\pi}\right)^{3/2}\exp(-\beta v^2) \tag{1}$$

with

$$\beta=\frac{m}{2kT},$$

where m is the molecule mass, T is the temperature, and k is the Boltzmann constant.

For given mean speed V and temperature, the air molecule flux $\dot{N}$ across a boundary surface with area A in a particular direction θ can be determined. The air molecule flux rate in boundary surface A is written as

$$\frac{\dot{N}}{A}=\frac{nV_{\mathrm{mp}}\{\exp(-q^2)+\sqrt{\pi}q[1+\mathrm{erf}(q)]\}}{2\sqrt{\pi}} \tag{2}$$

with

$$q=\frac{V}{V_{\mathrm{mp}}}\cos\theta,$$

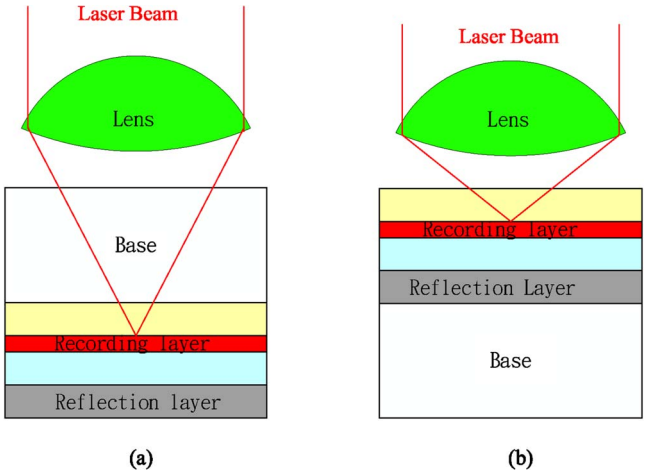

FIG. 1. Recording principle of (a) far-field and (b) near-field optical disk drives.

$$V_{\mathrm{mp}}=\sqrt{\frac{2kT}{m}},$$

where n is the number density (number of molecules in unit volume) and V_{mp} is the most probable speed.

By applying the particle flux conservation for each cell m (area A_m) at the inflow pressure boundary, the updated inflow streamwise velocity at cell m is computed as

$$(u_i)_m=\frac{\dot{N}_+-\dot{N}_-}{n_iA_m}, \tag{3}$$

where $\dot{N}_+$ and $\dot{N}_-$ are the particle flux into and out of the flow domain for cell m at the inflow pressure boundary using the latest updated $(u_i)_m$ and sampled streamwise velocity at each inflow boundary cell m with number density n_i in inflow stream and temperature T_i. At the outflow pressure boundary, a procedure similar to that used to treat inflow conditions is carried out for updating outflow streamwise velocity $(u_e)_m$ for each outflow boundary by applying the principle of particle flux conservation. Note that the outflow temperature for each cell interface is not given in advance and is set to the temperature sampled inside for each outflow boundary cell during simulation.

III. SIMULATION AND RESULTS

A. Near-field optical disk drives

Commercial optical disk drives such as CD-ROM and DVD-ROM read and record data by using the technology of far-field optics. The recording principle is shown in Fig. 1(a). However, the far-field optics is constrained by the optical property of diffraction limit and is difficult to further increase storage density. The architecture of far-field optical disk drives in reading and recording make the access time longer than hard disk drives. To overcome the bottleneck, near-field optical disk drives are under development to substitute far-field optical disk drives. By taking advantage of the near-field technology, the disk track pitch for near-field

This article is copyrighted as indicated in the article. Reuse of AIP content is subject to the terms at: http://scitation.aip.org/termsconditions. Downloaded to IP: 140.113.38.11 On: Thu, 01 May 2014 02:01:24

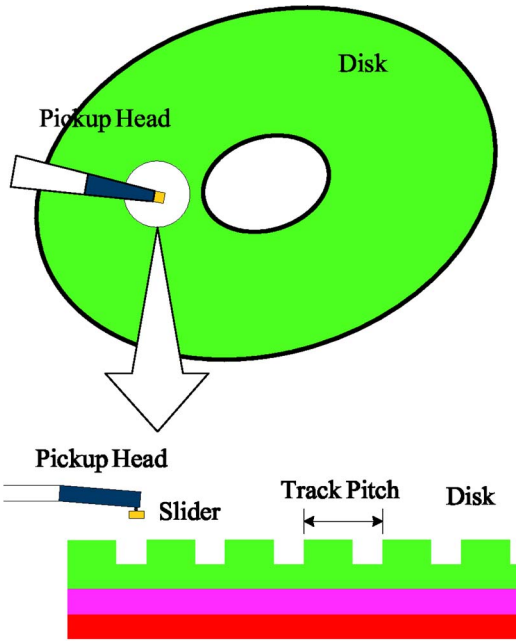

FIG. 2. Pickup head slider and near-field optical disk.

optical disk drives can become much smaller than CD-ROM or DVD-ROM and the storage density can hence be significantly increased.

Applying near-field optics to avoid the diffraction limitation, near-field optical disk drives can further reduce the light spot size to access smaller data track width and accomplish higher data recording density.[1] It adopts the structure of magnetic disk drives but replaces the magnetic pickup head slider by a near-field optical pickup head slider to maintain the space between the pickup head slider and disk within a near-field focusing length.[2] The recording density can thus be increased by optical resolution improvement. As the flight height is typically smaller than the mean free path of molecules in the air, i.e., 65 nm at STP, microscopic effects include slip length, air-surface accommodation, surface roughness, recording groove, etc. are important. The near-field optical disk drives are shown as Fig. 2. In order to overcome the diffraction limit, the flying height between the slider and recording layer in air-incidence phase change disk must be less than 100 nm. For lower distance between the slider and recording layer, the recording method is depicted in Fig. 1(b). Figure 3 shows a near-field optical disk with grooved surface, where grooves and lands constitute a trench-like feature of a rewritable optical disk. Before the optical disk records information, lands and grooves are used to define the track location. The pregroove has the following functions:

(1) sector configuration,
(2) stable tracking servo for reading and recording, and
(3) heat isolation for high-density recording.

The groove depth is prescribed as 50 nm. The widths of the groove and land are 100 and 200 nm, respectively. Unlike conventional optical disks, the recording layer of the near-field optical disk is on the disk surface. Hence, the recording tracks with the grooves and lands constitute disk roughness.

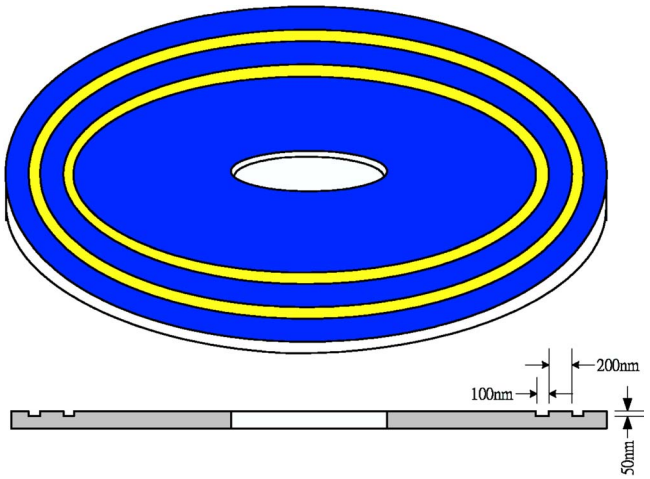

FIG. 3. Grooves and lands in near-field optical disk.

The geometry of the near-field optical disk is full of tracks on the disk surface although only two grooves are depicted in Fig. 3. The groove influence is shown between near-field optical disk and smooth disk.[12] The pressure is smaller when slider flies above the near-field optical disk than that when slider flies above the smooth disk. At such low flying height, the disk groove influence cannot be neglected. Hence, all the simulation in this study deals with the grooved near-field optical disk.

B. Modeling and simulation

Figure 4 shows a three-dimensional (3D) slider air bearing configuration. Figure 5 shows a slider with three rails that will be investigated in this simulation. A solid immersion lense (SIL) is treated as the third rail and it is installed at the higher pressure zone on the flat slider because the SIL density is larger than the slider density. The higher pressure zone on the flat slider is shown by Huang and Bogy.[7] The length L of the slider used in this simulation is prescribed as 4 μm and its width W is 3.3 μm. The height of rails is 0.7 μm. The pitch angle α is 0.01 rad.

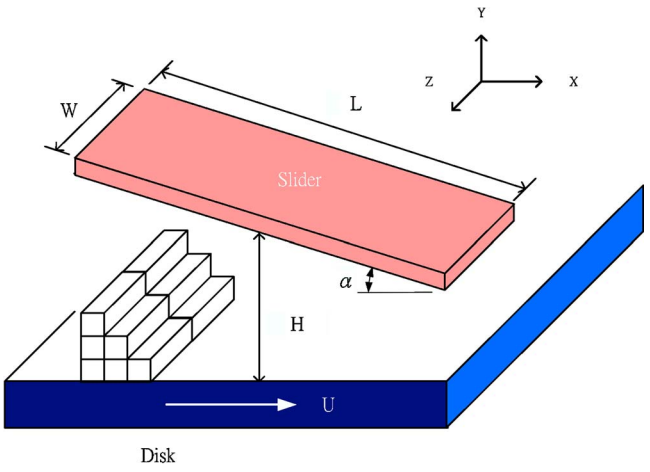

FIG. 4. Three-dimensional DSMC configuration.

This article is copyrighted as indicated in the article. Reuse of AIP content is subject to the terms at: http://scitation.aip.org/termsconditions. Downloaded to IP: 140.113.38.11 On: Thu, 01 May 2014 02:01:24

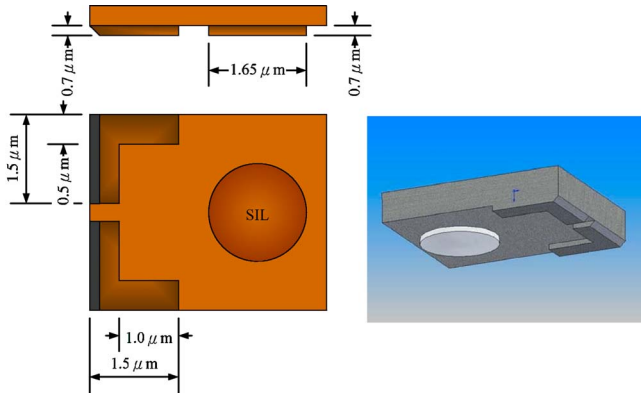

FIG. 5. Slider geometry.

To model a disk and a slider, the present model contains two solids in the control volume, where the upper and the lower surfaces are treated as solid. The other four faces of the control volume are treated as fluxing reservoirs in boundary condition definition. The four sides act as infinite with thermal equilibrium at temperature T_0 and ambient pressure P_0. The flow velocities in the reservoirs are such that the pressure on all four sides can be maintained at pressure P_0, but this study uses the air property at STP. Triangular elements are used in the solid surface grids. The points order defined for each triangular element is counterclockwise when looking from outside the surface. Figure 6 shows triangular elements of a parallelepiped. Orders of the points in two triangular elements are thus 1-3-2 and 1-4-3. The outward normal of the solid can be identified according to the right-hand rule by tracing the order of points in an element. For example, the arrow in element with node 1-3-2 shows the outward solid surface direction in Fig. 6. The arrow direction is determined by using the right-hand rule which traces the sequence nodes in elements.

To obtain detail pressure distribution, each length of triangular elements has to be shorter than the mean free path 65 nm of the air. The disk grooves depth is prescribed as

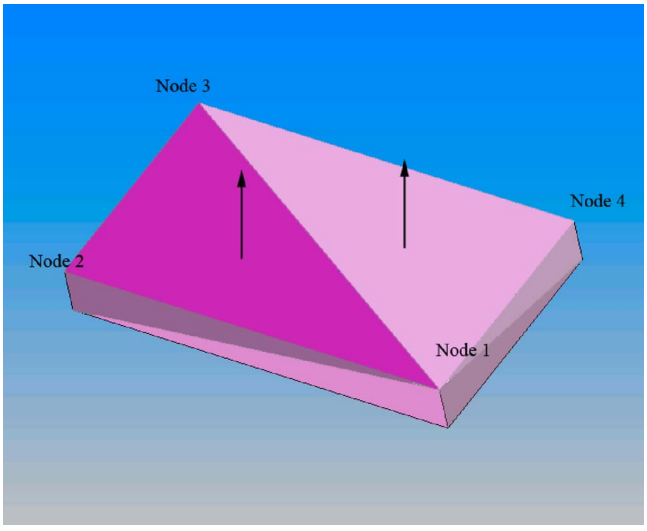

FIG. 6. Outward surface on solid is indicated as arrow directions.

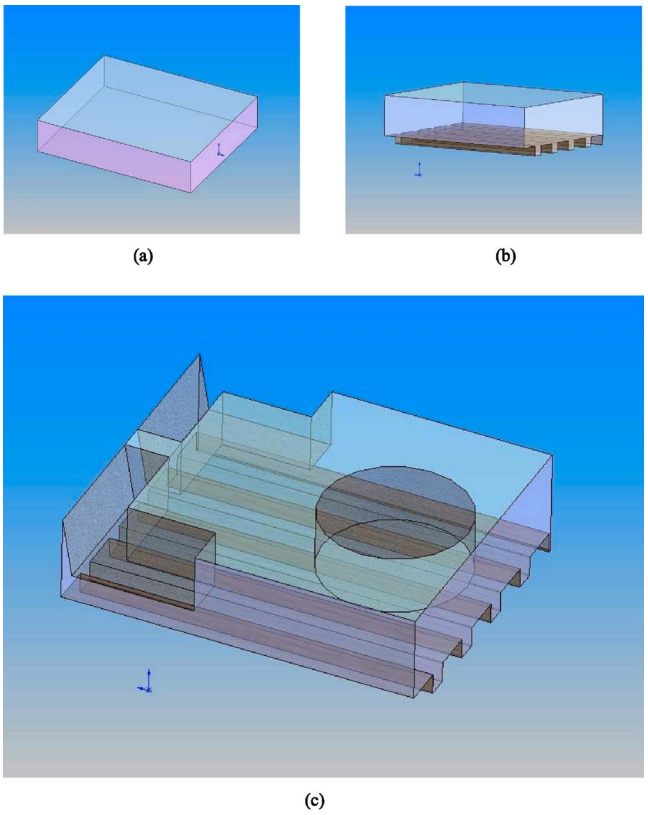

FIG. 7. (a) Original simulation region; (b) simulation region after disk surface is subtracted; and (c) simulation region after disk surface and slider bottom are subtracted.

50 nm in this study. To achieve the grid of the disk model, the disk groove depth should be divided by the length of triangular element with no remainder. As the slider bottom is symmetric with respect to its longitudinal axis, only half of the slider is required in the present model. Employing this symmetry reduces the model size and computation time.

The air under the slider is assumed to be dilute so that the potential energy of particles is negligible compared to the kinetic energy. As the real air is mixed by 4/5 nitrogen and 1/5 oxygen, it is complicated to deal with polyatomic molecules and mixed air using DSMC. Based on the previous assumptions, as the potential energy and the mean free path of air molecules are similar to those of argon, instead of real air molecules this study uses argon of temperature $T_0 = 0\ ^\circ\mathrm{C}$ and density $\rho = 1.78\ \mathrm{kg/m^3}$ in computing averaged quantities, including momentum and kinetic energy.

Figure 7(a) shows the entire simulation region filled with

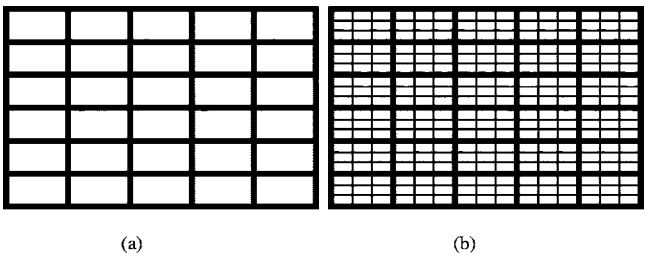

FIG. 8. (a) Parallelepipeds and (b) subparallelepipeds.

This article is copyrighted as indicated in the article. Reuse of AIP content is subject to the terms at: http://scitation.aip.org/termsconditions. Downloaded to IP: 140.113.38.11 On: Thu, 01 May 2014 02:01:24

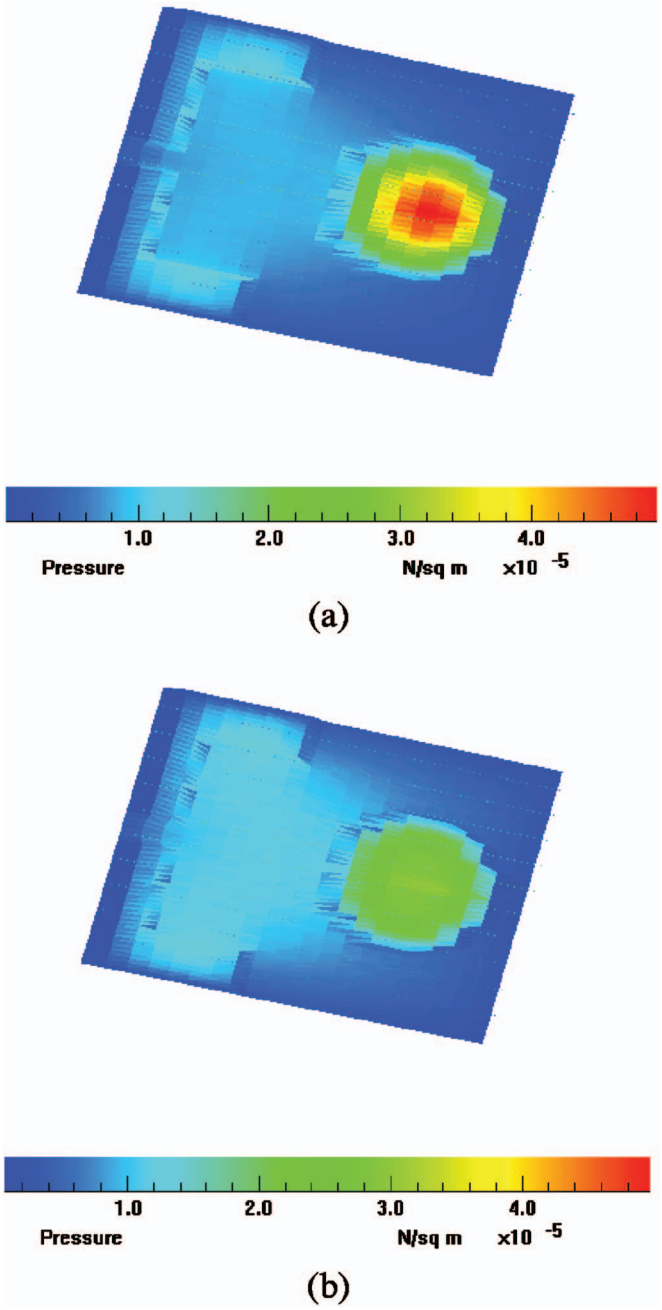

FIG. 9. (Color) Pressure distribution at 10 m/s airflow speed on slider bottom for slider flying heights of (a) 20 nm and (b) 30 nm.

argon and Fig. 7(b) shows the simulation region after subtraction of a disk. The final region used in simulation is shown as Fig. 7(c) that has subtracted a slider from Fig. 7(b). Except the solid region, the simulation region is filled with parallelepiped elements, which are filled with subparallelepiped elements. Figure 8(a) shows the parallelepiped elements and Fig. 8(b) shows subparallelepiped elements defined. In this study, the parallelepiped element size is 50 nm $\times$50 nm$\times$5 nm. Each parallelepiped element consists of four subparallelepiped elements, whose size are 25 nm $\times$25 nm$\times$5 nm.

C. Results

Figure 9(a) shows pressure distribution on the slider that

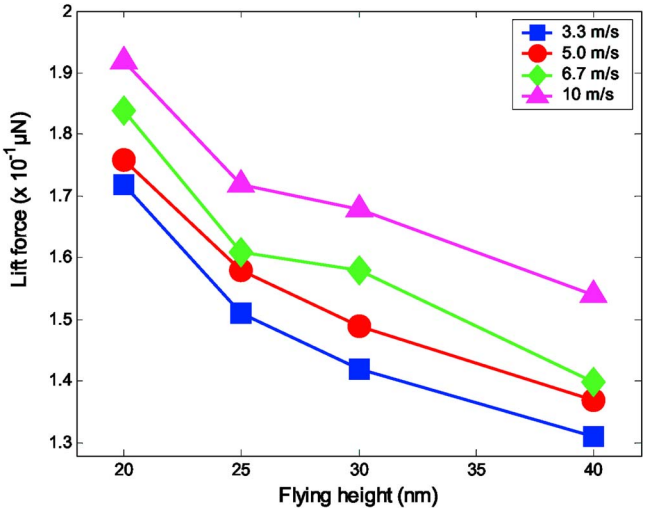

FIG. 10. Relationship among the lift force, flying height, and airflow speeds in track following.

may account for two situations. First, the slider keeps 20 nm flying height above a rotating near-field optical disk with 3600 rpm at the radial distance of 2.65 cm from the disk center. Second, the slider maintains 20 nm flying height above a rotating disk and the slider position along the radius direction depends on the disk speed to keep the airflow velocity constant. Figure 9(b) shows the slider pressure distribution in the same condition except the slider flying height of 30 nm. This section will show how disk speed affects lift force in track following or track seeking. In addition, this section also suggests where to tune the stable slider flying height so as to reach the near-field range by changing disk speed.

1. Track following

From the literature,[12] a slider flying above a near-field optical disk results in smaller pressure than flying above a smooth surface disk. The lift force for the same slider when flying above a disk with surface grooves is lower than when flying above smooth disks. How to obtain lift force large enough to maintain air bearing is critical in near-field optical disk drives for reading and writing. For near-field optics, smaller lift force generates lower flying height; i.e., shorter distance between the head and disk to realize higher resolution of reflective laser signals from a disk surface.

Figure 10 shows the relationship among the lift force, flying height, and disk speed. Faster speed results in larger lift force. Table I shows the relationship among the disk speed ω, airflow velocity v, and slider position r along the disk radial direction. This relationship in Table I is calculated from

$$v = r\omega. \tag{4}$$

According to Fig. 10, the higher speed leads to larger lift force in track following. The lift force at 25 nm height and 10 m/s speed is larger than that at 20 nm height and 3.3 m/s speed. As a consequence, faster disk speed can compensate lift force loss when flying higher.

This article is copyrighted as indicated in the article. Reuse of AIP content is subject to the terms at: http://scitation.aip.org/termsconditions. Downloaded to IP: 140.113.38.11 On: Thu, 01 May 2014 02:01:24

TABLE I. Slider radial position (cm) corresponding to disk speed and airflow velocity.

	Airflow velocity (m/s)			
Disk speed (rpm)	10.0	6.7	5.0	3.3
3600	2.65	1.76	1.32	⋯
2400	3.98	2.65	1.99	1.32
1800	⋯	3.54	2.65	1.76
1200	⋯	⋯	3.98	2.65

This study defines lift force stability as the ratio of lift force at arbitrary flow speed vs. lift force at flow speed of 3.3 m/s. If the force change percentage is close to 100%, it means that force variation is smaller and is treated as more stable. Figure 11 shows that lift force decrease percentage varies with both flying height and disk speed. Both this result and that presented by Huang and Bogy[7] show that lift force increases when the slider is closer to the disk whether the disk surface is grooved. Figure 11 depicts that at 10 m/s speed the lift force decrease rate is the smallest when flying height varies. Accordingly, the faster disk speed is advantageous for track following.

2. Track seeking

In track seeking at constant disk speed, the linear velocity varies with the radial position. Figure 12 shows that faster airflow generates larger lift force. In addition, the lower height yields a larger force. This result is similar to the results when a slider flies above a disk without grooves.[6] By comparing 20 and 25 nm flying heights, the lift force of the 20 nm flying height at any speed is larger than the largest lift force of 25 nm flying height at 10 m/s.

When the slider position changes at the same disk speed, the flow velocity at the head/disk interface changes. Table I lists the relationship among the disk speed, airflow velocity, and slider position along the disk radial direction when the disk diameter is 3.5 in.. Figure 13 shows the force change percentage relative to the 3.3 m/s velocity at each flying height when the slider position changes. A faster velocity results in a larger lift force. Therefore, flying lower is more stable when airflow velocity varies.

During track seeking, the slider position change makes the flow speed change. To maintain a stable flying height, minimizing lift force change is desired. Figure 13 depicts that flying lower experiences smaller lift force variation. Hence, in track seeking, it is advisable to fly as low as possible to increase stability.

In track seeking, variations of slider position along the disk radial direction lead to flow velocity changes. This relationship between slider position and flow velocity is shown in Table I. The air bearing results from airflow whose velocity change results in the bearing force change. In track seeking, there are two variations. One is the flow speed. The

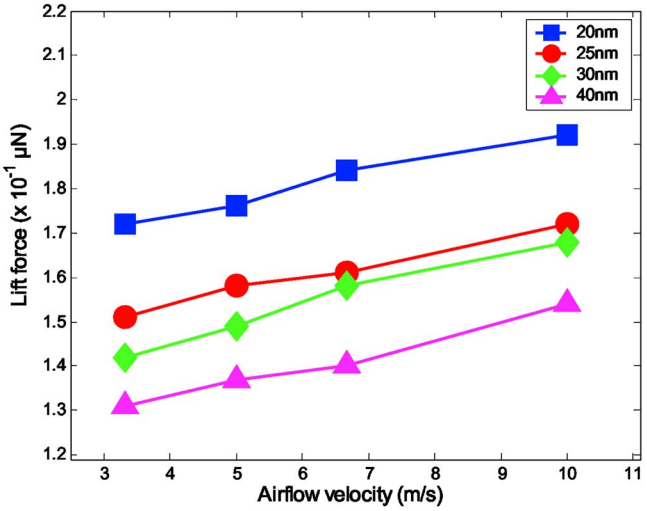

FIG. 12. Relationship among the lift force, flying height, and airflow speeds in track seeking.

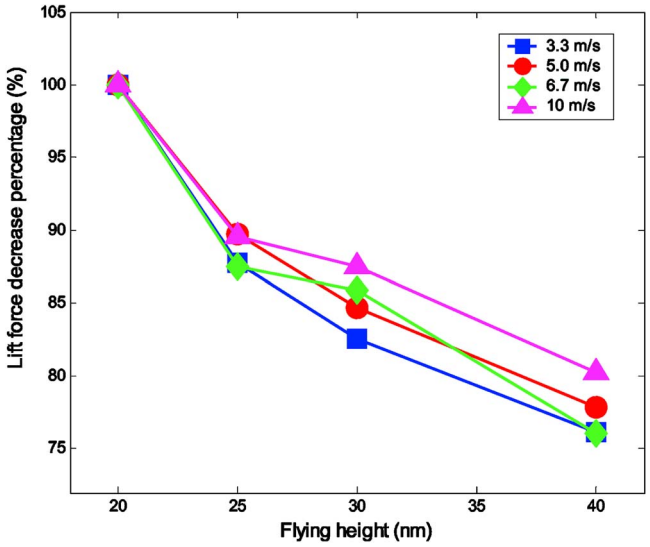

FIG. 11. Lift force decrease percentage when flying height increases in track following.

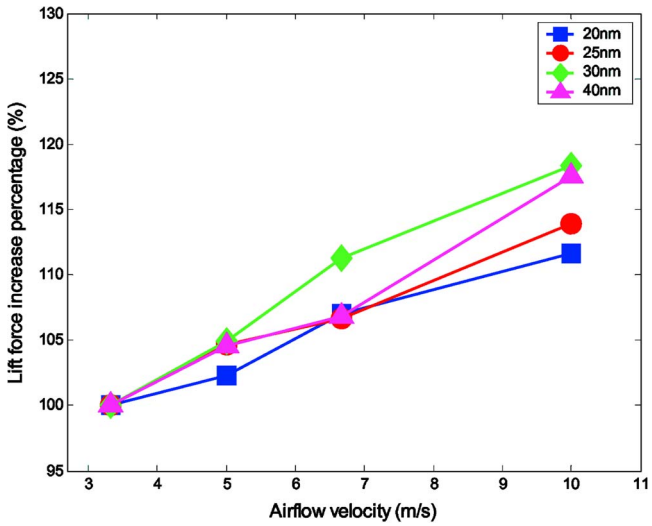

FIG. 13. Lift force increase percentage when airflow speed increases in track seeking.

This article is copyrighted as indicated in the article. Reuse of AIP content is subject to the terms at: http://scitation.aip.org/termsconditions. Downloaded to IP: 140.113.38.11 On: Thu, 01 May 2014 02:01:24

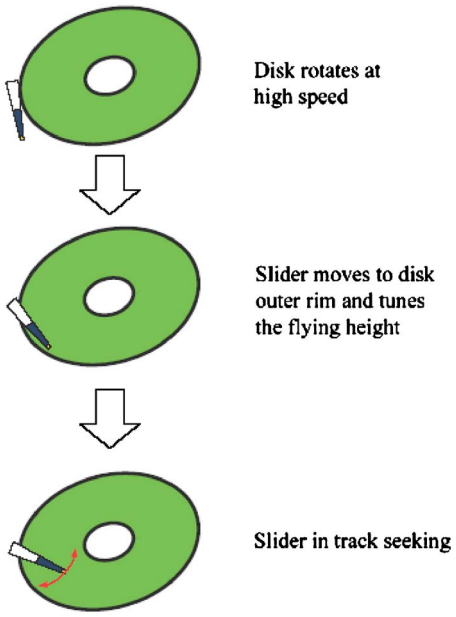

FIG. 14. A method for keeping the flying height within near field in track seeking.

other is the slider flying height change. Figure 12 shows that the lift force increases when the slider is closer to the disk. Hence, in track seeking, the slider seldom crashes even if the flow speed decreases. This study suggests to tune a stable flying height at the outer rim of the disk by changing the disk speed and the tuning steps are shown in Fig. 14. First, let the spindle motor rotate at a high speed and the slider move toward the disk. Second, let the slider move to reach a position above the disk outer rim and slow down the disk speed until the slider flies lower to lie within near-field range. When the slider moves closer to disk center at constant disk speed ω, the airflow slows down according to Eq. (4). However, the air bearing force will not be able to support the slider at the flying height. The slider hence further lowers its flying height to obtain new equilibrium among the lift force, pickup head elasticity, and gravitational force. Accordingly, the slider flying height can be maintained within the near field. Finally, move the slider to arrive at a target track on disk surface.

IV. CONCLUSION

This study investigates influence of the airflow velocity when a slider flies above a near-field optical disk. Computational results show that at the same flying height the higher flow velocity generates larger lift force. Faster airflow is more stable when the flying height changes. In track following, it is desired to maintain a faster velocity for stability. In track seeking, this study suggests that a stable flying height be obtained at an outer track on the disk by varying the disk speed, so as to maintain the slider flying height within the near field.

ACKNOWLEDGEMENT

This work was supported by "Photonics Science and Technology for Tera Era," Center of Excellence, National Science Council, Taiwan under Grant No. 94-E-009-009-PAE.

[1] T. D. Milster, "Near-field optics: A new tool for data storage," Proc. IEEE **88**, 1480 (2000).
[2] K. Ito, H. Saga, H. Nemoto, and H. Sukeda, "Advanced recording method using a near-field optics and the GMR head," in Proceedings of the Optical Data Storage, Conference Digest, Whistler, Canada, 2000, Vol. 14–17, p. 30.
[3] E. H. Kennard, *Kinetic Theory of Gases: With an Introduction to Statistical Mechanics* (McGraw-Hill, New York, 1938).
[4] A. Burgdorfer, "The influence of the molecular mean free path on the performance of hydrodynamic gas lubricated bearings," ASME J. Basic Eng. **81**, 94 (1959).
[5] G. A. Bird, *Molecular Gas Dynamics* (Clarendon, Oxford, 1976); *Molecular Gas Dynamics and the Direct Simulation of Gas Flows* (Oxford University Press, New York, 1994).
[6] F. J. Alexander, A. L. Garica, and B. J. Alder, "Direct simulation Monte Carlo for thin-film bearings," Phys. Fluids **6**, 3854 (1994).
[7] W. Huang and D. B. Bogy, "Three-dimensional direct simulation Monte Carlo method for slider air bearings," Phys. Fluids **9**, 1764 (1997).
[8] W. Huang and D. B. Bogy, "An investigation of slider air bearing with an asperity contact by a three-dimensional direct simulation Monte Carlo method," IEEE Trans. Magn. **34**, 1810 (1998).
[9] S. Fukui and R. Kaneko, "Analysis of ultra-thin gas film lubrication based on linearized Boltzmann equation: First report—derivation of a generalized lubrication equation including thermal creep flow," J. Tribol. **110**, 253 (1988).
[10] P. L. Bhatnagar, E. P. Gross, and M. Krook, "A model for collision processes in gases. I. Small amplitude processes in charged and neutral one-component systems," Phys. Rev. **94**, 511 (1954).
[11] N. Liu and E. Y. K. Ng, "The posture effects of a slider air bearing on is performance with a direct simulation Monte Carlo method," J. Magn. Magn. Mater. **11**, 463 (2001).
[12] H. C. Wang, T. S. Liu, and C. S. Chang, "Study of air bearing with grooved disk surface in near-field optical disk drives," IEEE Trans. Magn. **41**, 1047 (2005).

This article is copyrighted as indicated in the article. Reuse of AIP content is subject to the terms at: http://scitation.aip.org/termsconditions. Downloaded to IP: 140.113.38.11 On: Thu, 01 May 2014 02:01:24